Published in final edited form as:
Cancer Res. 2010 August 15; 70(16): 6629–6638. doi:10.1158/0008-5472.CAN-10-1616.

Dvl2 promotes intestinal length and neoplasia in the *Apc*^{Min} mouse model for colorectal cancer

Ciara Metcalfe[1,2], **Ashraf E. K. Ibrahim**[1], **Michael Graeb**[1], **Marc de la Roche**[1], **Thomas Schwarz-Romond**[1,3], **Marc Fiedler**[1], **Douglas J. Winton**[4], **Anthony Corfield**[5], and **Mariann Bienz**[1,6]

[1]MRC Laboratory of Molecular Biology, Hills Road, Cambridge CB2 0QH, UK

[4]CR-UK Cambridge Research Institute, Li Ka Shing Centre, Robinson Way, Cambridge CB2 0RE, UK

[5]Clinical Sciences at South Bristol, Bristol Royal Infirmary, Marlborough Street, Bristol BS2 8HW, UK

Abstract

APC mutations cause activation of Wnt/β-catenin signalling, which invariably leads to colorectal cancer. Similarly, overexpressed Dvl proteins are potent activators of β-catenin signalling. Screening a large tissue microarray of different staged colorectal tumours by immunohistochemistry, we found that Dvl2 has a strong tendency to be overexpressed in colorectal adenomas and carcinomas, in parallel to nuclear β-catenin and Axin2 (a universal transcriptional target of Wnt/β-catenin signalling). Furthermore, deletion of *Dvl2* reduced the intestinal tumor numbers in a dose-dependent way in the *Apc*^{Min} model for colorectal cancer. Interestingly, the small intestines of *Dvl2* mutants are shortened, reflecting in part a reduction of their crypt diameter and cell size. Consistent with this, mTOR signalling is highly active in normal intestinal crypts where Wnt/β-catenin signalling is active, and activated mTOR signalling (as revealed by staining for phosphorylated 4E-BP1) serves as a diagnostic marker of *Apc*^{Min} mutant adenomas. Inhibition of mTOR signalling in *Apc*^{Min} mutant mice by RAD001 (everolimus) reduces their intestinal tumour load, similarly to *Dvl2* deletion. mTOR signalling is also consistently active in human hyperplastic polyps, and has a significant tendency for being active in adenomas and carcinomas. Our results implicate Dvl2 and mTOR in the progression of colorectal neoplasia and highlight their potential as therapeutic targets in colorectal cancer.

Keywords

Dvl2 signalling; mTOR signalling; phosphorylated 4E-BP1; *Apc*^{Min} mouse model; colorectal cancer

INTRODUCTION

Most colorectal cancers are initiated by hyperactivation of the Wnt/β-catenin pathway in the intestinal epithelium, typically by loss-of-function mutations of the *APC* tumour suppressor (1, 2). APC is a negative regulator of β-catenin: it binds to Axin, to promote the phosphorylation of β-catenin by glycogen synthase kinase 3β (GSK3β), thus earmarking it

[6]Corresponding author: MRC Laboratory of Molecular Biology, Hills Road, Cambridge CB2 0QH, UK, mb2@mrc-lmb.cam.ac.uk.
[2]Present address: Genentech, South San Francisco, CA 94080, USA
[3]Present address: EMBO, Meyerhofstr. 1, 69117 Heidelberg, Germany

Europe PMC Funders Author Manuscripts

for proteasomal degradation (3). APC truncations such as those typically found in colorectal cancer lack their Axin-binding domain, and therefore retain only partial function (4); thus, β-catenin accumulates in the cytoplasm and nucleus where it binds to TCF factors to operate a transcriptional switch. *Apc* mutations in mice also initiate intestinal tumorigenesis (5), and the transcriptional programme activated by APC loss resembles that of the normal intestinal crypts, which comprise the intestinal stem cell compartment (2). One of the key APC effector genes in normal crypts and tumorigenesis is *c-myc* (6).

Loss of APC function mimics β-catenin activation by Wnt signals in normal cells, which critically depends on Dishevelled (Dvl) (7): upon Wnt stimulation, Dvl binds to and recruits Axin to the plasma membrane by virtue of its polymerising activity (8, 9), thus assembling signalosomes that also contain Frizzled receptor and LRP6 co-receptor and promoting the phosphorylation of the LRP6 cytoplasmic tail (10, 11). The latter acts as a direct inhibitor of GSK3β (12, 13), which allows unphosphorylated β-catenin to accumulate and trigger a transcriptional switch, much like *APC* loss. Notably, if Dvl is expressed at high levels, it potently activates β-catenin, independently of Wnt stimulation: it recruits Axin into cytoplasmic signalosomes (8, 9) and inhibits GSK3β through LRP6 phosphorylation (14).

In binding to Axin, Dvl blocks the activity of the Axin-APC complex in downregulating β-catenin; if overexpressed, Dvl could thus synergise with a partially functional Axin-APC complex, and further promote Wnt/β-catenin pathway activity. This is the case in *Drosophila*, where *dishevelled* is essential for Wnt pathway activity in hypomorphic *APC* mutant embryos (15). The same could be true in colorectal cancer cells which carry hypomorphic *APC* mutations (4), which delete the Axin-binding domain from APC, and thus allow only indirect association of the two proteins through β-catenin (16); indeed, these cancer cells could be particularly sensitive to Dvl expression levels, and their β-catenin hyperactivation might reflect both their Dvl signalling activity and their *APC* loss. If so, Dvl and its signalling partners (which include several kinases (7)), could have potential as targets for therapeutic intervention.

To examine the possible role of Dvl in colorectal cancer, we screened a large tissue microarray (TMA) of colorectal tumour samples, and found that Dvl2 has a strong tendency to become overexpressed during the tumour progression. Furthermore, we show that lowering the dose of *Dvl2* reduces the numbers of intestinal tumours in the Apc^{Min} mouse model, indicating a tumour-promoting role of Dvl2 in the intestine. We also discovered that *Dvl2*−/− mice have shortened intestines, and we present evidence that this reflects partly fewer intestinal crypts, and partly reduced crypt diameters, suggesting that Dvl2 may promote crypt cell growth. Consistent with this, we show that crypts exhibit high levels of phosphorylated 4E-BP1 (p4E-BP1), a key read-out of activated mTOR signalling which promotes cell growth (17), consistent with earlier results (18). Indeed, we find high p4E-BP1 levels to be a diagnostic marker for nascent polyps and larger intestinal tumours of Apc^{Min} mutant mice, and we confirm that inhibition of this pathway by the rapamycin-like inhibitor RAD001 reduces the tumour numbers in this model (18). Importantly, we find that mTOR signalling is highly active in human hyperplastic polyps, and also within a subset of adenomas and colorectal carcinomas, indicating the therapeutic potential of mTOR inhibitors in colorectal cancer.

MATERIALS AND METHODS

Mouse models

Animal care and procedures were performed in accordance with the standards set by the United Kingdom Home Office. *Dvl2*+/− mice (19, 20) were back-crossed into a C57BL/6 background (the genetic background of $Apc^{Min/+}$ (5)) for 4 successive generations (whereby

the final cross was with *Apc*$^{Min/+}$), and compound *Apc*$^{Min/+}$*Dvl2*+/+, *Apc*$^{Min/+}$*Dvl2*−/+ and *Apc*$^{Min/+}$*Dvl2*−/− mutants were generated from a back-cross of *Apc*$^{Min/+}$ *Dvl2*−/+ males with *Dvl2*−/+ females.

Tissue analysis and adenoma scoring

Organ sizes were determined by weighing or, in the case of the small intestine, by measuring the distance between stomach and caecum in intact dissected intestines. Tumours were scored in dissected intestines (including the colon) of 120 day-old mice, as described (21). For immunohistochemistry of intestinal preparations, previously described procedures were followed, including fixation by methacarn or formalin (22). Staining was done with α-p4E-BP1 (Cell Signaling Technology) or other antibodies (see below). Crypt-enriched tissue lysates were generated as described (23) (see also supplementary information).

siRNA knockdown, Western blot and real-time quantitative PCR (RT-qPCR) analysis

siRNA-mediated depletion of Dvl2, TOPFLASH luciferase reporter assays, Western blot and RT-qPCR analyses (**Suppl. Fig.** 1 **&** 3) were done as described (8, 24) (for details of cell lines used, see supplementary information). To detect endogenous Dvl2 (Fig. 1B; suppl. Fig. 1C), a rabbit antiserum was generated against human Dvl2 (amino acids 78-250), affinity-purified and characterised in overexpression and siRNA-mediated depletion experiments (M.G., not shown), as described (8, 25).

Colorectal tumour samples

Tissue samples for Western blots (suppl. Fig. 1C) were collected from patients undergoing elective surgery for colorectal resections in accordance with standard procedures (26); ethical approval for this collection was granted by the United Bristol Hospital Trust Research and Development Ethical Committee (SU/2005/2114 and 05/Q2006/164). For analysis by immunohistochemistry (**Fig.** 1 **&** 6; suppl. Fig. 2), two TMAs were constructed from multiple (2-4) replicate tissue cores from 64 patients undergoing colectomy resections for colorectal cancer at Addenbrookes Hospital, Cambridge (Ibrahim et al., submitted); ethical approval was obtained from the Cambridgeshire Local Research Ethics Committee (04/Q0108/125 and 06/Q0108/307). Samples were selected on the basis of availability of paraffin blocks with adequate cellularity. Haematoxylin & eosin-stained (H&E) slides of all cases were reviewed, marked and used to guide the sampling from morphologically representative regions of the tissue blocks. 5 μm sections were obtained from paraffin-embedded blocks, and deparaffinized and rehydrated with xylene and alcohol. Antigen retrieval was performed with EDTA buffer (pH 9.0) at 100°C for 20 min. The following antibodies were used: affinity-purified α-Dvl2 (1:50); α-β-catenin (1:200; BD Transduction Laboratories); α-Axin2 (1:500; Abcam); α-pS6 (1:100; Cell Signaling Technology). A commercially available α-Dvl2 antiserum was also tested on some samples (1:100; AB5972, Millipore), with similar results as those obtained with our affinity-purified antibody. Antibody detection was done by streptavidin-biotin labelling, and visualization with di-amino benzidine chromagen (Dako). All slides were scored blinded to clinical outcome and other experimental data; strength of staining was scored semi-quantitatively as negative (0), weakly positive (1), moderately positive (2) or strongly positive (3). β-catenin staining was scored as percentage of positively labelled nuclei.

RESULTS

Endogenous Dvl2 is expressed at high levels in various colorectal cancer cell lines (suppl. Fig. 1A). Furthermore, Dvl2 depletion by siRNA reduced the β-catenin-specific transcription (measured by TOPFLASH luciferase reporter assays (27)) by ~50% (suppl. Fig. 1B). This suggested that Dvl2 contributes to the β-catenin hyperactivation in colorectal

cancer cells, and prompted us to examine the Dvl2 expression levels in colorectal tumours. Screening total protein lysates from a small set of human colorectal carcinomas (n=24) by Western blot analysis, we found that the Dvl2 levels were elevated in approximately one third of the carcinomas compared to their resection margin controls (suppl. Fig. 1C). We thus proceeded to screen a TMA of 393 tissue cores from 64 patients presenting with colorectal cancer, including subsets of matched normal mucosa, hyperplastic and adenomatous polyps and staged colorectal carcinomas, by staining them with affinity-purified antibody against Dvl2, and compared this to antibody staining against Axin2, a well-established universal Wnt/β-catenin target gene (28), and β-catenin itself which accumulates in cell nuclei during the progression of colorectal cancer (29). We found that the number of β-catenin-positive nuclei increased in a step-wise fashion from normal tissue to carcinoma (Fig. 1A, D), with the majority of carcinomas showing significantly increased nuclear β-catenin compared with normal tissue (Wilcoxon Rank Sum, $p < 2.2e-16$). Nuclear β-catenin was also significantly increased within hyperplastic polyps compared with normal tissue (Wilcoxon Rank Sum, $p = 5.817e-06$), and even more so in adenomas (Wilcoxon Rank Sum, $p = 8.774e-05$) (Fig. 1A), indicative of their high β-catenin-mediated transcriptional activity, due to their *APC* mutations typically observed in >80% of adenomas (29). These results support the widely-held view that *APC* mutation alone can cause nuclear accumulation of β-catenin, and argue against the notion that the latter requires, in addition, an activating KRAS mutation (30). As expected from the nuclear β-catenin, Axin2 has a highly significant tendency to be overexpressed in hyperplastic polyps and adenomas compared with normal tissue (Wilcoxon Rank Sum, $p = 6.333e-07$ and 3.655e-05, respectively), which increases even further in carcinomas (Wilcoxon Rank Sum, $p = 7.444e-05$) (Fig. 1B, D). In turn, the pattern of increasing Axin2 expression through the tumour progression from benign to malignant is closely mirrored by Dvl2, whose levels increase also significantly (Wilcoxon Rank Sum, $p = 3.953e-12$) from moderate in hyperplastic polyps and adenomas to high in carcinomas, where it exhibits a punctate cytoplasmic staining pattern (Fig. 1C, D; suppl. Fig. 2). Indeed, there is a remarkable correlation between the Dvl2 and Axin2 expression levels in the different tumour stages (Pearson's correlation, $r = 0.5394386$, $p < 2.2e-16$), indicating that Dvl2 may be upregulated, along with Axin2, in response to *APC* loss from the onset of colorectal tumorigenesis. Consistent with this, we found that stimulation of HEK293 cells by Wnt3a causes an increase of endogenous Dvl2 protein levels, although its transcript levels remain unchanged (suppl. Fig. 3). Thus, Dvl2 can be upregulated post-transcriptionally upon Wnt-stimulation, providing a possible explanation why this protein accumulates in cancer cells whose Wnt/β-catenin pathway is hyperactive.

Next, we tested whether Dvl2 contributes to the β-catenin-dependent intestinal tumorigenesis in the Apc^{Min} model, i.e. whether *Dvl2* loss would suppress the intestinal tumour load in these mutants. $Apc^{Min/+}$ (referred to as *Min*/+) mice develop numerous intestinal tumours over the course of 3-4 months (5), likely reflecting a β-catenin-dependent transcriptional switch in the intestinal epithelium (22, 31). *Dvl2* homozygosity causes various embryonic and perinatal defects, however 50% of these *Dvl2*−/− mice survive and develop into apparently normal healthy adults (19). We thus generated *Min*/+ *Dvl2*+/− and *Min*/+ *Dvl2*−/− compound mutant mice, and found that the adenoma numbers of 120 day-old mice were reduced significantly in a *Dvl2* dose-dependent manner, i.e. noticeably in *Dvl2*+/− ($p = 0.038$, 2-tailed *t*-test; Fig. 2A), and even more so in *Dvl2*−/−, on average to ~55% of their matched *Dvl2*+/+ controls ($p = 0.0065$, 2-tailed *t*-test; Fig. 2A). The disease onset in *Dvl2*−/− may also be slightly delayed compared to the other two experimental cohorts, as revealed by Kaplan-Meier survival plots (Fig. 2B): although this delay is not statistically significant, due to the high intrinsic variation of disease onset, the observed delay may nevertheless be indicative of the reduced tumour numbers in some of the animals. Our results identify *Dvl2* as a contributor to the intestinal tumour incidence in this mouse

model. Notably, the *Dvl2*−/− mice retain the function of two Dvl paralogs, *Dvl1* and *Dvl3*, each of which shares overlapping redundant functions with *Dvl2* (double mutants being embryonic lethal (19, 20)). Therefore, the functional contribution of *Dvl2* to intestinal neoplasia (Fig. 2) is likely an underestimate of the overall Dvl function in this process. Indeed, we detect transcripts of both paralogs, *Dvl1* and *Dvl3*, in lysates of wt and *Dvl2*−/− mutant intestinal epithelia (suppl. Fig. 4). Technical difficulties with the available antibodies prevented us from assessing the Dvl protein levels in intestinal lysates, but our transcript data suggest that the total Dvl function may be reduced by approximately half in the *Dvl2*−/− mutant intestine.

While scoring tumours, we noticed that the small intestines of the *Dvl2*−/− mice were significantly shorter than their controls ($p < 0.0001$, *t*-test; Fig. 3A). This gut shortening to 75% ± 2% (mean ± *s.d.*) of normal length is fully penetrant and highly consistent between individuals. It is also observed in a normal *Min*+/+ background, and is already manifest at 8 days of age (Fig. 3B). The circumference of the *Dvl2*−/− mutant intestines appears normal (6-7 mm in both wt and mutants, upon opening up and flattening out), though the accuracy of these measurements is limited to ± 0.5 mm. The body weights of the mutants are also normal, and so are their organ weights (Table 1), possibly because each of the organs assessed expresses at least one of the two Dvl2 paralogs at high levels (32). Thus, the small intestine appears to be particularly vulnerable to the loss of Dvl2. Evidently, intestinal length and tumour numbers represent functional read-outs that are sensitive to partial Dvl loss.

To examine the underlying defect of the ‘short gut’ phenotype, we examined longitudinal sections through wt and *Dvl2*−/− mutant small intestines, both of which revealed a normal overall tissue architecture (Fig. 4A-C). However, the diameters of the mutant intestinal crypts appeared slightly reduced (Fig. 4A, arrows; also compare **B, C**). To quantify this effect, we measured the diameters of individual crypts (n = 111, 4 mice per genotype) selected on the basis of their orientation parallel to the sectional plane, but blinded to the genotype, and found that the crypt diameters are reduced in the *Dvl2*−/− samples, on average to 93% of their matched wt samples (Fig. 4D; Table 1). Although relatively small, this reduction is highly statistically significant ($p < 0.0001$, *t*-test). It likely contributes to the shortened intestines of the *Dvl2*−/− mutants, but does not fully account for this phenotype. Indeed, we estimate that the reduced crypt diameters could account for ~30% of the total length reduction (2.6/9 cm) seen in 4 month-old mice. The remainder is most likely due to fewer crypts: based on our measurements of gut length, circumference and crypt diameter, we estimate that the total numbers of crypts in the small intestine are reduced to between 93% and 75% of the wt. Notably, each crypt contains a small number of long-lived stem cells with tumour-forming potential (33), so lower crypt numbers in the *Dvl2*−/− mutants could explain at least partly why they develop fewer tumours (although we could not detect a significant reduction of BrdU-incorporating cells in the mutants; suppl. Fig. 5).

The crypt diameter can be taken as a measure of cell size, specifically of the apicobasal axis of individual crypt cells, visualised by staining of the membrane-associated β-catenin (Fig. 4B, C), whose length seemed reduced in *Dvl2*−/− mutant crypts (not shown), suggesting that Dvl2 may promote cell size (or growth) in intestinal crypts. Cell size is controlled primarily by the mTOR signalling pathway, and its well-established S6 kinase (S6K) effector arm that results in phosphorylation of ribosomal protein S6 (pS6) (17). mTOR can be activated by a number of growth factors and kinases (17), e.g. by Ras signalling (34), but also by Wnt/Dvl signalling, which was reported to affect cell size in tissue culture (35). Interestingly, high levels of pS6 staining have been observed in normal murine intestinal crypts and in *Apc* mutant intestinal tumours; furthermore, *mTORC1* transcription depends on β-catenin in *APC* mutant colorectal cancer cells (18).

We thus asked whether the reduced crypt diameters in the *Dvl2* mutants might be due to reduced mTOR signalling, by staining histological sections of intestinal preparations with antibodies against pS6. We thus confirmed that the crypts and adenomas are generally positive for this mTOR signalling read-out (18) (suppl. Fig. 6), although the staining was somewhat variable, and depended on the type of fixation. We thus chose to examine the phosphorylation of 4E-BP1 (p4E-BP1), an equally well-established read-out of mTOR signalling that controls translational initiation through eIF-4E (17), and thought to be important in oncogenesis (34). These p4E-BP1 stainings turned out to be far more robust: we observe highly restricted p4E-BP1 staining throughout normal crypts, apparently in every cell (Fig. 5A). Likewise, every single adenoma shows p4E-BP1 staining in most if not all cells (Fig. 5B). Indeed, we used p4E-BP1 staining to identify nascent polyps, appearing as tubes within a single villus as previously described (36) (Fig. 5C). To confirm their identification, we stained adjacent sections for β-catenin, which was nuclear throughout the polyp, in every cell (Fig. 5D), again, arguing against the notion that APC loss is insufficient to cause nuclear accumulation of β-catenin (30). Thus, mTOR signalling is activated with full penetrance throughout normal crypts, and in every adenoma. Indeed, the p4E-BP1 staining is a diagnostic marker for adenomas in the Apc^{Min} model. Given that virtually all adenomas in *Apc* mutant mice show *Apc* inactivation (36), this strongly supports the notion that the activation of mTOR signalling in adenomas is a direct consequence of β-catenin-dependent transcription due to *Apc* loss (18). Notwithstanding this, we were unable to detect a consistent reduction of pS6 or p4E-BP1 staining in normal crypts or adenomas of *Dvl2*−/− mice compared to their controls (suppl. Fig. 7A, B; not shown), although we found a slight reduction of pS6 levels in crypt-enriched intestinal lysates from *Dvl2*−/− versus *Dvl2*+/− littermate controls by Western blot analysis (suppl. Fig. 7C). Given the redundancy problem with Dvl2 paralogs, this is perhaps not surprising: indeed, Wnt/β-catenin signalling was not detectably reduced in embryos even upon simultaneous knock-out of two *Dvl* paralogs (19, 20). Also, a subtle attenuation of mTOR signalling in *Dvl2*−/− mutants would be difficult to detect by immunohistochemistry.

Notably, both *Dvl2* loss and mTOR inhibition have comparable tumour-suppressive effects in the Apc^{Min} model: oral administration of the mTOR inhibitor RAD001 to Apc^{Min} mice reduces their intestinal tumour numbers by ~50% (suppl. Fig. 8A), similar to *Dvl2* homozygosity (Fig. 2A), although again, we cannot detect a robust reduction of mTOR signalling in adenomas of treated mice compared to their controls, by staining these with p4E-BP1 or pS6 antibodies (suppl. Fig. 8B, C; not shown). Our findings with RAD001 confirm earlier results from this mTOR inhibitor in a different *Apc* mutant model (18), and reinforce the conclusion that the high mTOR signalling levels observed in crypts or adenomas promote the intestinal tumorigenesis driven by *Apc* loss.

Given the fully penetrant activation of mTOR signalling in murine adenomas, we also screened our TMA of human colorectal tumours with pS6 antibody (and with p4E-BP1 antibody, though this did not produce reliable staining of these samples). While we observe very low pS6 signals in normal intestinal mucosa (Fig. 6A, left), hyperplastic polyps consistently show high levels of pS6 staining, apparently in every single cell (Fig. 6A, right), thus mirroring the murine adenomas. mTOR signalling is therefore a hallmark of these polyps, and may be a direct consequence of activating mutations in their KRAS/BRAF signalling pathway, as often found in these polyps (37). Indeed, the cells in the hyperplastic polyps are visibly larger than those in the adjacent normal epithelium (Fig. 6A, B), suggesting that their growth is stimulated by their mTOR signalling. Adenomas and carcinomas also have a high tendency to show strong pS6 staining (Fig. 6C), though on average, their probability of elevated mTOR activity is lower than that of the hyperplastic polyps, with approximately one and two thirds of all adenomas and carcinomas, respectively, showing robust pS6 staining (Fig. 6D). Basically the same was found with

cyclin D1 (not shown), another mTOR signalling target whose translational stimulation requires phosphorylated 4E-BP1 (38). Thus, the mTOR signalling pathway has a significant tendency to remain active throughout the progression of colorectal cancer.

DISCUSSION

Our work provides two lines of evidence for a tumour-promoting role of Dvl2 in colorectal cancer. Firstly, the Dvl2 protein levels are elevated through the cancer progression, closely correlating with Axin2 protein levels that increase in parallel (Fig. 1). Therefore, Dvl2 may be upregulated, like Axin2, as a direct result of APC loss. However, while the upregulation of Axin2 is likely to be due to transcriptional stimulation by β-catenin (28), that of Dvl2 may occur at the post-transcriptional level (suppl. Fig. 3), although we note that the transcript levels of Dvl2 are also elevated >2x in response to *Apc* inactivation throughout the intestinal epithelium (6). Importantly, given that Dvl2 causes β-catenin accumulation upon overexpression, in the absence of a Wnt signal (9), this implies that the high Dvl2 levels in colorectal carcinomas contribute to, or maintain, the high levels of (nuclear) β-catenin at advanced stages. Secondly, *Dvl2* deficiency reduced the tumour load in Apc^{Min} mutant mice (Fig. 2), providing experimental evidence for its tumour-promoting role in this mouse model for colorectal cancer. The reduced tumour numbers in the *Dvl2*−/− mutants could be partly due to reduced crypt numbers, and partly to reduced crypt cell growth (see below). Notably, overexpression of Dvl paralogs has been observed in cervical carcinomas (39), and seems to contribute to the pathogenesis of mesothelioma and small cell lung cancer (40, 41). Furthermore, Dvl proteins appear to become hyperactive in colorectal cancer cells due to transcriptional silencing of their inhibitor DACT3 (42). These results, together with our own work, highlight the potential of Dvl2 as a therapeutic target in cancers driven by hyperactive Wnt/β-catenin signalling.

Perhaps our most interesting result was that *Dvl2* deficiency reduces the length of the small intestine. This mutant phenotype results in part from a reduction of the crypt numbers, but also from a reduced crypt diameter, itself a measure of crypt cell size. Given Dvl's normal role in transducing Wnt signals to β-catenin, it is possible that some or all aspects of this mutant phenotype are a consequence of attenuated β-catenin-mediated transcription. In particular, the narrowed crypts may reflect attenuated mTOR signalling, given that (1) mTOR signalling commonly regulates cell size (17), (2) mTOR signalling is high in normal crypts, and (3) signalling through this pathway is stimulated by Dvl and β-catenin, through transcriptional stimulation of *mTORC1* (18, 35). Our inability to detect a robust reduction of mTOR signalling in the *Dvl2*−/− mutant crypts could be due to the above-mentioned redundancy problem; also, we may not have analysed mTOR signalling during the critical time window, or in the critical subset of cells, responsible for the narrow crypt and/or short gut phenotype. Interestingly, a small cell phenotype was also observed upon conditional deletion of *c-myc* (43), a key transcriptional target of hyperactive Wnt/β-catenin signalling in murine and human intestinal epithelial cells (21, 44), indicating that Wnt/β-catenin signalling could impact on cell size. Indeed, Wnt/Dvl and mTOR signalling might act synergistically on common targets (sequentially, or in parallel): intriguingly, many of the reported transcriptional targets of Wnt/β-catenin signalling (including c-myc, cyclin D1, VEGF, survivin, MMP9) have independently been identified as translational targets of the mTOR/eIF-4E pathway (e.g. (34, 45)). Furthermore, although *cyclin D1* is thought to be a transcriptional target of β-catenin (2), cyclin D protein rather than transcript levels are upregulated in the murine intestine upon *Apc* inactivation (46), and in Wnt-stimulated tissue culture cells (35). Thus, the transcriptional changes induced by Wnt/Dvl signalling may generally be accompanied by mTOR-dependent translational changes.

Europe PMC Funders Author Manuscripts

Alternatively, it is also possible that the shortened intestines in the *Dvl2*−/− mutants reflect one of the β-catenin-independent ('non-canonical') Dvl functions (7). We note that gut elongation is compromised in *Wnt5a* and *Ror2* knock-out mice, along with other non-canonical Wnt signalling defects, though in both mutants, the short gut phenotypes result from gross morphological abnormalities in the early embryonic midgut primordium, such as convergent extension defects (47, 48).

It is striking that the mTOR signalling pathway is upregulated not only in normal murine intestinal crypts and in all intestinal adenomas (18) (Fig. 5B,C; **suppl. Fig.** 6-8), but also in human hyperplastic polyps, with a significant tendency of being active also in adenomas and colorectal carcinomas (Fig. 6C,D), strongly supporting the notion that mTOR has potential as a therapeutic target in colorectal cancer (18). Indeed, we extended the results of these authors, showing efficacy of the mTOR inhibitor RAD001 in reducing the intestinal tumour load in a different *Apc* model. mTOR inhibitors have been in use clinically as immunosuppressants for many years, and have begun to show great promise in cancer treatment, in particular of renal cell carcinomas, but also in other types of solid tumours (49). Our findings, together with previous results (18), provide evidence for a future application of these inhibitors in colorectal cancers, at least in those pre-screened for mTOR signalling read-outs, and possibly also in young familial adenomatous polyposis patients, carriers of *APC* germ-line mutations, which develop thousands of adenomas before reaching adulthood (50).

Supplementary Material

Refer to Web version on PubMed Central for supplementary material.

Acknowledgments

We thank Tony Wynshaw-Boris for the *Dvl2* knock-out strain, and Owen Samson for technical advice regarding the analysis of mouse intestines, and for discussion. We further thank Tracey Butcher and her animal staff, Paul Sylvester, Rob Longman and Paul Durdey for their assistance. M. F. and M. de la R. were supported by Cancer Research UK (grant no C7379/A8709 to M.B.), A. E. K. I. by a Clinician Scientist Fellowship from Cancer Research UK. Core support was provided by the Medical Research Council (U1051030200000101).

REFERENCES

1. Polakis P. Wnt signaling and cancer. Genes Dev. 2000; 14:1837–51. [PubMed: 10921899]
2. Clevers H. Wnt/β-catenin signaling in development and disease. Cell. 2006; 127:469–80. [PubMed: 17081971]
3. Bienz M, Clevers H. Linking colorectal cancer to Wnt signaling. Cell. 2000; 103:311–20. [PubMed: 11057903]
4. Albuquerque C, Breukel C, van der Luijt R, et al. The 'just-right' signaling model: APC somatic mutations are selected based on a specific level of activation of the β-catenin signaling cascade. Hum Mol Genet. 2002; 11:1549–60. [PubMed: 12045208]
5. Su LK, Kinzler KW, Vogelstein B, et al. Multiple intestinal neoplasia caused by a mutation in the murine homolog of the APC gene. Science. 1992; 256:668–70. [PubMed: 1350108]
6. Sansom OJ, Meniel VS, Muncan V, et al. Myc deletion rescues Apc deficiency in the small intestine. Nature. 2007; 446:676–9. [PubMed: 17377531]
7. MacDonald BT, Tamai K, He X. Wnt/β-catenin signaling: components, mechanisms, and diseases. Dev Cell. 2009; 17:9–26. [PubMed: 19619488]
8. Schwarz-Romond T, Metcalfe C, Bienz M. Dynamic recruitment of axin by Dishevelled protein assemblies. J Cell Sci. 2007; 120:2402–12. [PubMed: 17606995]
9. Schwarz-Romond T, Fiedler M, Shibata N, et al. The DIX domain of Dishevelled confers Wnt signaling by dynamic polymerization. Nat Struct Mol Biol. 2007; 14:484–92. [PubMed: 17529994]

10. Bilic J, Huang YL, Davidson G, et al. Wnt induces LRP6 signalosomes and promotes dishevelled-dependent LRP6 phosphorylation. Science. 2007; 316:1619–22. [PubMed: 17569865]
11. Zeng X, Huang H, Tamai K, et al. Initiation of Wnt signaling: control of Wnt coreceptor Lrp6 phosphorylation/activation via frizzled, dishevelled and axin functions. Development. 2008; 135:367–75. [PubMed: 18077588]
12. Piao S, Lee SH, Kim H, et al. Direct inhibition of GSK3β by the phosphorylated cytoplasmic domain of LRP6 in Wnt/β-catenin signaling. PLoS ONE. 2008; 3:e4046. [PubMed: 19107203]
13. Wu G, Huang H, Garcia Abreu J, He X. Inhibition of GSK3 phosphorylation of β-catenin via phosphorylated PPPSPXS motifs of Wnt coreceptor LRP6. PLoS One. 2009; 4:e4926. [PubMed: 19293931]
14. Metcalfe C, Mendoza-Topaz C, Mieszczanek J, Bienz M. Stability elements in the LRP6 cytoplasmic tail confer efficient signalling upon DIX-dependent polymerization. J Cell Sci. 2010; 123:1588–99. [PubMed: 20388731]
15. McCartney BM, Dierick HA, Kirkpatrick C, et al. Drosophila APC2 is a cytoskeletally-associated protein that regulates wingless signaling in the embryonic epidermis. J Cell Biol. 1999; 146:1303–18. [PubMed: 10491393]
16. Hart MJ, de los Santos R, Albert IN, Rubinfeld B, Polakis P. Downregulation of β-catenin by human Axin and its association with the APC tumor suppressor, β-catenin and GSK3β. Curr Biol. 1998; 8:573–81. [PubMed: 9601641]
17. Ruvinsky I, Meyuhas O. Ribosomal protein S6 phosphorylation: from protein synthesis to cell size. Trends Biochem Sci. 2006; 31:342–8. [PubMed: 16679021]
18. Fujishita T, Aoki K, Lane HA, Aoki M, Taketo MM. Inhibition of the mTORC1 pathway suppresses intestinal polyp formation and reduces mortality in ApcDelta716 mice. Proc Natl Acad Sci U S A. 2008; 105:13544–9. [PubMed: 18768809]
19. Hamblet NS, Lijam N, Ruiz-Lozano P, et al. Dishevelled 2 is essential for cardiac outflow tract development, somite segmentation and neural tube closure. Development. 2002; 129:5827–38. [PubMed: 12421720]
20. Etheridge SL, Ray S, Li S, et al. Murine dishevelled 3 functions in redundant pathways with dishevelled 1 and 2 in normal cardiac outflow tract, cochlea, and neural tube development. PLoS Genet. 2008; 4:e1000259. [PubMed: 19008950]
21. Sansom OJ, Berger J, Bishop SM, Hendrich B, Bird A, Clarke AR. Deficiency of Mbd2 suppresses intestinal tumorigenesis. Nat Genet. 2003; 34:145–7. [PubMed: 12730693]
22. Sansom OJ, Reed KR, Hayes AJ, et al. Loss of Apc in vivo immediately perturbs Wnt signaling, differentiation, and migration. Genes Dev. 2004; 18:1385–90. [PubMed: 15198980]
23. Flint N, Cove FL, Evans GS. A low-temperature method for the isolation of small-intestinal epithelium along the crypt-villus axis. Biochem J. 1991; 280:331–4. [PubMed: 1747105]
24. de la Roche M, Worm J, Bienz M. The function of BCL9 in Wnt/β-catenin signaling and colorectal cancer cells. BMC Cancer. 2008; 8:199. [PubMed: 18627596]
25. Semenov MV, Snyder M. Human dishevelled genes constitute a DHR-containing multigene family. Genomics. 1997; 42:302–10. [PubMed: 9192851]
26. Sylvester PA, Myerscough N, Warren BF, et al. Differential expression of the chromosome 11 mucin genes in colorectal cancer. J Pathol. 2001; 195:327–35. [PubMed: 11673830]
27. Korinek V, Barker N, Morin PJ, et al. Constitutive transcriptional activation by a β-catenin-Tcf complex in APC−/− colon carcinoma. Science. 1997; 275:1784–7. [PubMed: 9065401]
28. Lustig B, Jerchow B, Sachs M, et al. Negative feedback loop of Wnt signaling through upregulation of conductin/axin2 in colorectal and liver tumors. Mol Cell Biol. 2002; 22:1184–93. [PubMed: 11809809]
29. Fodde R, Brabletz T. Wnt/β-catenin signaling in cancer stemness and malignant behavior. Curr Opin Cell Biol. 2007; 19:150–8. [PubMed: 17306971]
30. Phelps RA, Chidester S, Dehghanizadeh S, et al. A two-step model for colon adenoma initiation and progression caused by APC loss. Cell. 2009; 137:623–34. [PubMed: 19450512]
31. Foley PJ, Scheri RP, Smolock CJ, Pippin J, Green DW, Drebin JA. Targeted suppression of β-catenin blocks intestinal adenoma formation in APC Min mice. J Gastrointest Surg. 2008; 12:1452–8. [PubMed: 18521697]

32. Tsang M, Lijam N, Yang Y, Beier DR, Wynshaw-Boris A, Sussman DJ. Isolation and characterization of mouse dishevelled-3. Dev Dyn. 1996; 207:253–62. [PubMed: 8922524]
33. Barker N, Ridgway RA, van Es JH, et al. Crypt stem cells as the cells-of-origin of intestinal cancer. Nature. 2009; 457:608–11. [PubMed: 19092804]
34. Mamane Y, Petroulakis E, Rong L, Yoshida K, Ler LW, Sonenberg N. eIF4E--from translation to transformation. Oncogene. 2004; 23:3172–9. [PubMed: 15094766]
35. Inoki K, Ouyang H, Zhu T, et al. TSC2 integrates Wnt and energy signals via a coordinated phosphorylation by AMPK and GSK3 to regulate cell growth. Cell. 2006; 126:955–68. [PubMed: 16959574]
36. Oshima M, Oshima H, Kitagawa K, Kobayashi M, Itakura C, Taketo M. Loss of Apc heterozygosity and abnormal tissue building in nascent intestinal polyps in mice carrying a truncated Apc gene. Proc Natl Acad Sci U S A. 1995; 92:4482–6. [PubMed: 7753829]
37. O'Brien MJ. Hyperplastic and serrated polyps of the colorectum. Gastroenterol Clin North Am. 2007; 36:947–68. viii. [PubMed: 17996799]
38. Averous J, Fonseca BD, Proud CG. Regulation of cyclin D1 expression by mTORC1 signaling requires eukaryotic initiation factor 4E-binding protein 1. Oncogene. 2008; 27:1106–13. [PubMed: 17724476]
39. Okino K, Nagai H, Hatta M, et al. Up-regulation and overproduction of DVL-1, the human counterpart of the Drosophila dishevelled gene, in cervical squamous cell carcinoma. Oncol Rep. 2003; 10:1219–23. [PubMed: 12883684]
40. Uematsu K, He B, You L, Xu Z, McCormick F, Jablons DM. Activation of the Wnt pathway in non small cell lung cancer: evidence of dishevelled overexpression. Oncogene. 2003; 22:7218–21. [PubMed: 14562050]
41. Uematsu K, Kanazawa S, You L, et al. Wnt pathway activation in mesothelioma: evidence of Dishevelled overexpression and transcriptional activity of β-catenin. Cancer Res. 2003; 63:4547–51. [PubMed: 12907630]
42. Jiang X, Tan J, Li J, et al. DACT3 is an epigenetic regulator of Wnt/β-catenin signaling in colorectal cancer and is a therapeutic target of histone modifications. Cancer Cell. 2008; 13:529–41. [PubMed: 18538736]
43. Muncan V, Sansom OJ, Tertoolen L, et al. Rapid loss of intestinal crypts upon conditional deletion of the Wnt/Tcf-4 target gene c-Myc. Mol Cell Biol. 2006; 26:8418–26. [PubMed: 16954380]
44. van de Wetering M, Sancho E, Verweij C, et al. The β-catenin/TCF-4 complex imposes a crypt progenitor phenotype on colorectal cancer cells. Cell. 2002; 111:241–50. [PubMed: 12408868]
45. Graff JR, Konicek BW, Carter JH, Marcusson EG. Targeting the eukaryotic translation initiation factor 4E for cancer therapy. Cancer Res. 2008; 68:631–4. [PubMed: 18245460]
46. Sansom OJ, Reed KR, van de Wetering M, et al. Cyclin D1 is not an immediate target of β-catenin following Apc loss in the intestine. J Biol Chem. 2005; 280:28463–7. [PubMed: 15946945]
47. Cervantes S, Yamaguchi TP, Hebrok M. Wnt5a is essential for intestinal elongation in mice. Dev Biol. 2009; 326:285–94. [PubMed: 19100728]
48. Yamada M, Udagawa J, Matsumoto A, et al. Ror2 is required for midgut elongation during mouse development. Dev Dyn. 2010; 239:941–53. [PubMed: 20063415]
49. Konings IR, Verweij J, Wiemer EA, Sleijfer S. The applicability of mTOR inhibition in solid tumors. Curr Cancer Drug Targets. 2009; 9:439–50. [PubMed: 19442061]
50. Lal G, Gallinger S. Familial adenomatous polyposis. Semin Surg Oncol. 2000; 18:314–23. [PubMed: 10805953]

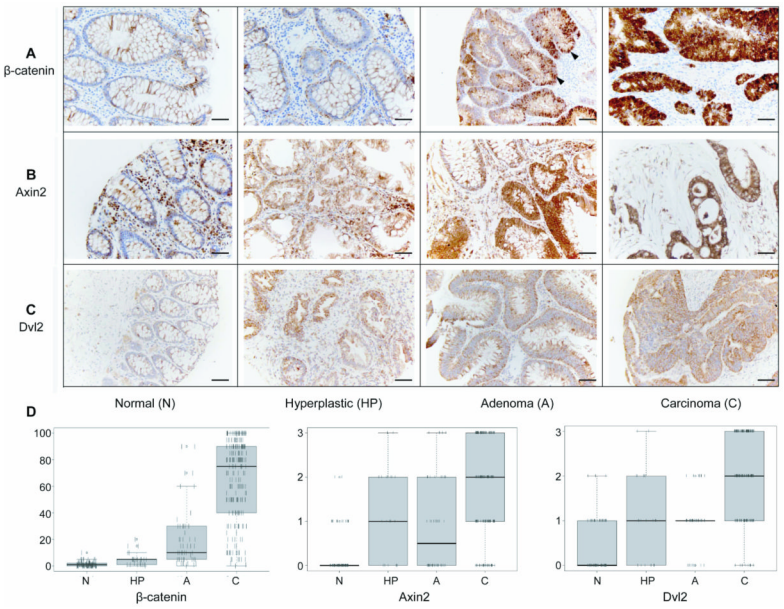

Fig. 1. Dvl2 and Axin2 are overexpressed in colorectal tumours

(A-C) Immunohistochemical staining of TMA cores of normal colonic tissues, hyperplastic polyps, adenomatous polyps and adenocarcinomas, as indicated underneath panels, fixed and stained with antibodies, as indicated on the left; arrowheads point to nuclear β-catenin. Scale bars, 100 μm. (**D**) Boxplots representing the TMA scoring results; each individual tissue core is represented by a vertical line; boxes straddle the 25th to 75th percentiles (thick horizontal line, 50th percentile); outliers are above or below thin horizontal lines (90th and 10th percentiles, respectively).

Europe PMC Funders Author Manuscripts

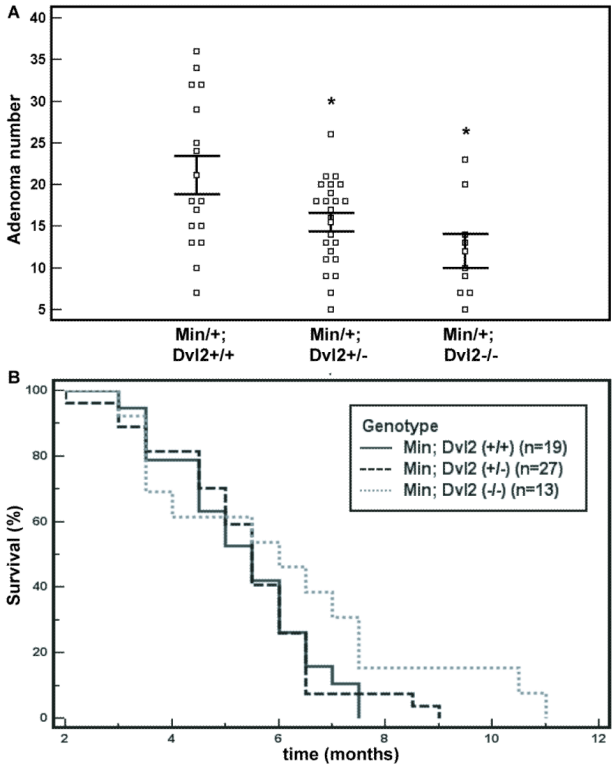

Fig. 2. *Dvl2* deficiency reduces the intestinal tumour numbers in Apc^{Min} mice

(A) Adenoma counts in 120 day-old Apc^{Min} *Dvl2*+/+ (n = 16), Apc^{Min} *Dvl2*−/+ (n = 23) and Apc^{Min} *Dvl2*−/− (n = 9) mice; each square represents one mouse, horizontal lines show standard error of the mean; * indicates statistical significance. (**B)** Kaplan-Meier survival plots of all three cohorts.

Europe PMC Funders Author Manuscripts

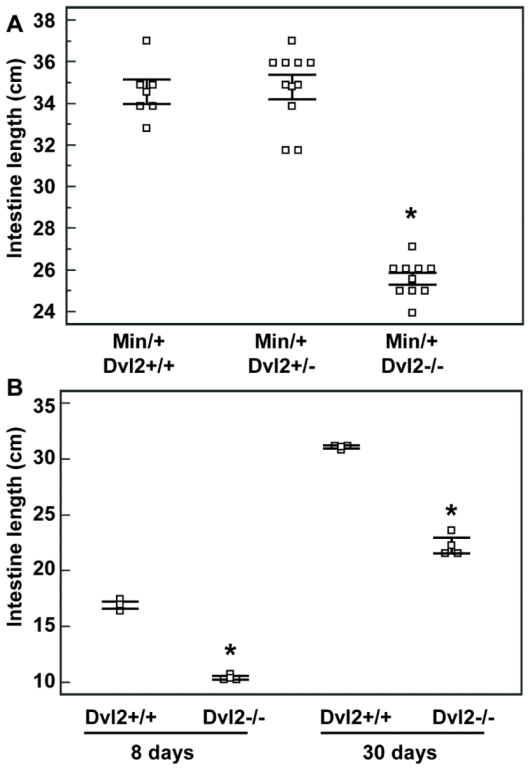

Fig. 3. *Dvl2* mutants have short guts

Length measurements of the small intestines from *Dvl2*−/− and littermate controls (n > 3) at (**A**) 120 days, (**B**) 8 or 30 days after birth; statistical significance and symbols as in Fig. 2 (see also text).

Europe PMC Funders Author Manuscripts

Europe PMC Funders Author Manuscripts

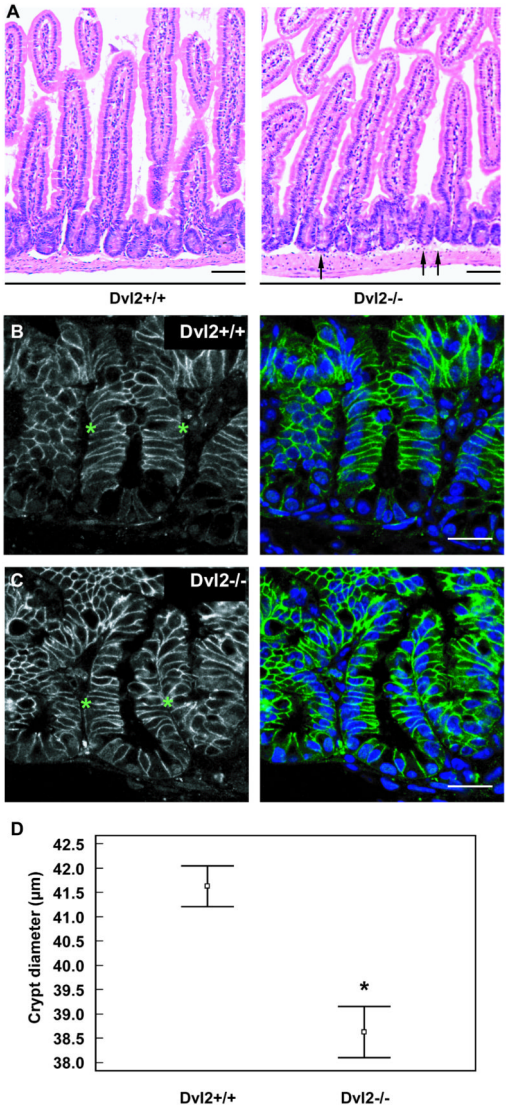

Fig. 4. *Dvl2* mutants have reduced crypt diameters

(**A-C**) Longitudinal sections through the small intestine of a 2 month-old *Dvl2*−/− and littermate controls, (**A**) after H&E staining; arrows point to individual narrow crypts in the mutant. Scale bars, 100 μm; **(B, C)** immunofluorescence images, revealing decreased crypt diameters in *Dvl2*−/− compared to littermate controls, as measured along apicobasal axis of intestinal crypt cells (between asterisks); blue, DAPI staining; green, α-β-catenin staining; scale bars, 25 μm. **(D)** Measurements of crypt diameters (n = 111) from sections as shown in **(A)** (4 mice per genotype); small squares indicate the mean, and lines standard error of the mean; *, statistical significance.

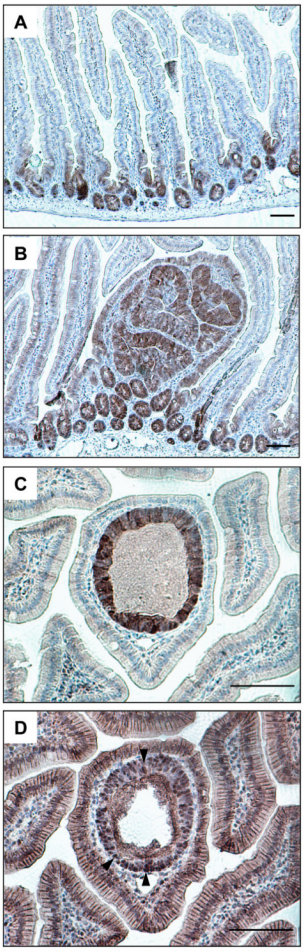

Fig. 5. mTOR signalling is induced in murine intestinal crypts, and in nascent polyps

(**A, B**) Longitudinal sections through (**A**) normal crypts and (**B**) a small adenoma in the small intestine of 120 day-old Apc^{Min} mice, stained for p4E-BP1; strong signals are characteristic for normal crypts and adenomas. (**C, D**) High-magnification views of adjacent sections through a nascent polyp in a 120 day-old Apc^{Min} mouse, stained for (**C**) p4E-BP1, and (**D**) β-catenin, revealing nuclear β-catenin in every cell (arrowheads). Scale bars, 100 μm.

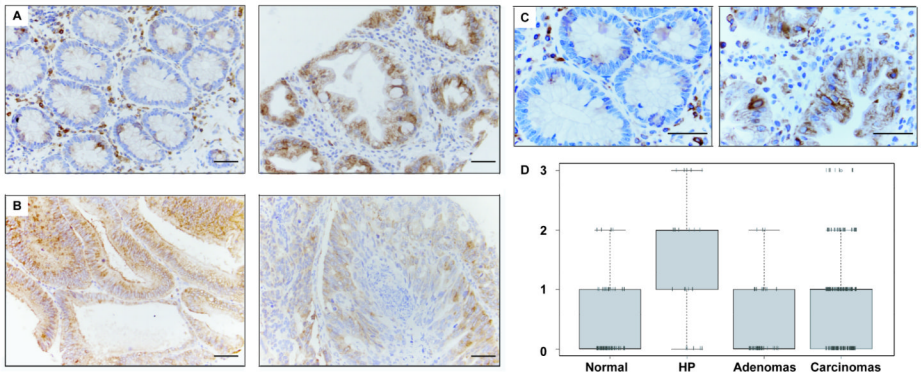

Fig. 6. mTOR signalling is elevated in human colorectal tumours

(**A-C**) TMA cores of (**A**) normal mucosa (left) and matched hyperplastic polyp (right), and (**B**) adenoma (left) compared to adenocarcinoma (right), stained for pS6; (**C**) high magnification views, as in (**A**), of a different matched sample pair. (**D**) Boxplots of the α-pS6 TMA scoring results, as in Fig. 1D.

Europe PMC Funders Author Manuscripts

Europe PMC Funders Author Manuscripts

Table 1

Intestine lengths, crypt diameters and organ weights of wt and Dvl2 mutant mice

Measurements of small intestines (n >10 per genotype) and organ weights (n = 3 per genotype) from 120 day-old mice. Crypt diameters (n = 132, 3 mice per genotype) were calculated with AxioVision software (Zeiss); ± represents standard error.

	Dvl2 (+/+)	Dvl2 (+/−)	Dvl2 (−/−)	Dvl2(−/−)/Dvl2 (+/+) (percent)	P value (t test)
Small intestine (cm)	34.1 ± 0.70	34.9 ± 0.55	25.5 ± 0.26	75	P < 0.005
Crypt width (μm)	41.63 ± 0.42	-	38.63 ± 0.53	93	P < 0.005
Spleen (g)	0.09 ± 0.00	-	0.09 ± 0.01	100	-
Kidneys (g)	0.26 ± 0.01	-	0.29 ± 0.03	111	-
Liver (g)	1.11 ± 0.12	-	1.10 ± 0.27	99	-
Heart (g)	0.12 ± 0.00	-	0.12 ± 0.00	100	-